Tellus SERIES B CHEMICAL AND PHYSICAL METEOROLOGY
PUBLISHED BY THE INTERNATIONAL METEOROLOGICAL INSTITUTE IN STOCKHOLM

Tellus (2011), 63B, 448–458
Printed in Singapore. All rights reserved

TELLUS

Doppler lidar studies of heat island effects on vertical mixing of aerosols during SAMUM–2

By RONNY ENGELMANN[1,*], ALBERT ANSMANN[1], STEFAN HORN[1], PATRIC SEIFERT[1], DIETRICH ALTHAUSEN[1], MATTHIAS TESCHE[1], MICHAEL ESSELBORN[2], JULIA FRUNTKE[3], KIRSTEN LIEKE[4], VOLKER FREUDENTHALER[5] and SILKE GROSS[5], [1]*Leibniz Institute for Tropospheric Research, Permoserstraße 15, 04318 Leipzig, Germany;* [2]*European Southern Observatory (ESO), Karl-Schwarzschild-Straße 2, 85748 Garching, Germany;* [3]*German Meteorological Service, Regional- und Seewetterzentrale Hamburg, Bernhard-Nocht-Straße 76, 20359 Hamburg, Germany;* [4]*Institute for Applied Geosciences, Technical University Darmstadt, Schnittspahnstraße 9, 64287 Darmstadt, Germany;* [5]*Meteorological Institute, Ludwig-Maximilians-Universität, Theresienstraße 37, 80333 Munich, Germany*

(Manuscript received 23 November 2010; in final form 12 May 2011)

ABSTRACT

A wind Doppler lidar was deployed next to three aerosol lidars during the SAMUM–2 campaign on the main island of Cape Verde. The effects of the differential heating of the island and the surrounding ocean and the orographic impact of the capital island Santiago and the small island on its luv side, Maio, are investigated. Horizontal and vertical winds were measured in the disturbed maritime boundary layer and compared to local radiosoundings. Lidar measurements from the research aircraft Falcon and a 3-D Large Eddy Simulation (LES) model were used in addition to study the heating effects on the scale of the islands. Indications are found that these effects can widely control the downward mixing from greater heights to the surface of African aerosols, mainly Saharan dust and biomass-burning smoke, which were detected in a complex layering over the Cape Verde region.

1. Introduction

It is well known that flat heat islands in the stable maritime environment can cause strong convection and vertical mixing of aerosols, trace gases and momentum (Carbone et al., 2000; Savijärvi and Matthews, 2004; Minda et al., 2010). The islands of Cape Verde with their pronounced orography with mountains of 1000–3000 m height may further disturb the long-range transport of aerosols advected from west Africa because they act as mechanical obstacles (e.g. Carlis et al., 2010). As a result of flow alternation such islands may modify the ocean–atmosphere interaction depending on meteorological conditions. For example, surface aerosol concentration or even oceanic fertilization, that is, the amount of dust and iron sedimenting into the sea water, could be modified. Furthermore, the study of the island effects on the generation of boundary-layer (BL) turbulence depending on the wind direction can be important for airport traffic control at small oceanic islands like Cape Verde.

Within the second Saharan Mineral Dust Campaign (SAMUM–2) in early 2008 a supersite was set up in the southeast of the Cape Verde island Santiago at the airport of the capital city of Praia (Ansmann et al., 2011). Various ground-based remote sensing systems (lidars, photometers, and an infrared radiometer), in situ instruments for chemical, microscopic, and optical particle characterization, and a radiosonde station were operated at the site. Additionally, the Falcon research aircraft of the DLR (Deutsches Zentrum für Luft und Raumfahrt) was operated in order to sample aerosol particles and measure their properties throughout the dust and smoke layers on a regional scale (Weinzierl et al., 2011; Petzold et al., 2011).

A wind Doppler lidar was deployed to measure almost continuously the vertical wind component in aerosol layers as well as in clouds (Ansmann et al., 2009a). An important goal was the characterization of turbulent motions over the islands. In this study of the impact of the island on the air flow we include the measurements from the High Spectral Resolution Lidar (HSRL, Esselborn et al., 2008) aboard the Falcon aircraft. A number of flight legs crossing the island parallel (downstream) and orthogonal to the main wind direction were performed. The HSRL proved to be especially useful to study the horizontal extent and

*Corresponding author.
e-mail: ronny@tropos.de
DOI: 10.1111/j.1600-0889.2011.00552.x

variability of the atmospheric aerosol layers over the Cape Verde region.

Several studies are reported in the literature regarding the disturbance of horizontal and vertical airflow by islands. Savijärvi and Matthews (2004) studied the effect of small islands (5–40 km in diameter) with a two-dimensional non-linear model using the example of the tropical island of Nauru (5 km in diameter) and compared their results to aircraft measurements. They used two model setups, the first of which neglected large-scale winds, in order to investigate the sea-breeze strength. In a second setup they added horizontal winds typical for islands in the trade-wind zone. Gravity waves developed and they found a plume which extended 20 km downstream of the island and which was 0.3 K warmer and 0.5 g kg^{-1} drier than the undisturbed maritime boundary layer (MBL). Small islands in the tropics can furthermore initiate mesoscale convective systems. Carbone et al. (2000) showed results of the Maritime Continent Thunderstorm Experiment. They studied the role of the relatively flat Tiwi Islands north of Australia for the formation of Hector, an intense, consistent, and local thunderstorm which forms because of complex interaction between sea-breeze fronts and convectively generated cold pools. In contrast to flat islands, Carlis et al. (2010) carried out detailed simulations of the Maui Vortex. This closed-circulation vortex is formed in the lee of the mountains (3055 and 1764 m height) over the Hawaiian island in the summer trade-wind regime as a result of orographic blocking of the flow. However, exclusive simulations are not sufficient to understand the heat island effects. For example, Minda et al., (2010) describe the evolution of the island BL and the initiation of clouds over Okinawa Island, Japan, during conditions with weak synoptic forcing. It was shown that only the combination of radar observations and cloud-resolved modelling enabled the authors to understand the island BL evolution. They found the formation of convectively generated horizontal rolls, a convergence zone over the island and sea-breeze fronts which generated cumulus streets over the island. They also compared model results for the flat and the orographic island with elevations of up to 500 m. The formation of the convective rolls were found to be very similar for both cases and only somewhat disturbed by the orography in the northern part of the island.

The aim of this paper is to study possible heat island effects and how the island BL development can influence the stable lower-tropospheric stratification in the northeasterly trade-wind flow. We focus on the possibility of downward mixing of biomass-burning aerosol, dust and maritime aerosol, towards the ocean surface. The paper is organized as follows. First, the field site at Praia airport and the applied instruments are introduced in Section 2. In Section 3 we describe the general meteorological situation during SAMUM–2 and show that horizontal wind profiles obtained from Doppler lidar scans are in good agreement with those from radiosoundings. In Section 4 we present the setup of a Large Eddy Simulation (LES) which was used to place the measurements at Praia into a greater scale. The measurements are shown in Section 5. First, we describe a situation where the air was transported for more than 30 km over a land mass before it reached the measurement site. In contrast, a second case is presented in which the air masses in low altitude range (0–500 m) were advected first over the small neighbouring island of Maio and then directly, and only 2 km over land, towards the measurement site. A summary and concluding remarks are given in Section 6.

2. Field site and instrumentation

The Cape Verde islands are located in the Atlantic Ocean approximately 700 km from the west African coast of Senegal. The archipelago consists of 10 islands in an area of 250 × 250 km^2. Figure 1 shows an orographic map of Santiago (991 km^2), the largest island of the Republic of Cape Verde. The measurement site (14.94° N, 23.48° W) at the airport is close to Praia, the capital city of Cape Verde in the very south of Santiago. The island extends about 50 km from north to south and 30 km from east to west. The highest mountain of Santiago is the Pico da Antónia with a height of almost 1400 m. Upwind of the lidar site, to the northeast, hills with top heights of only 100 m are found. About 40 km to the northeast of the measurement site and upwind of the typical wind direction the small island of Maio (269 km^2) is situated.

Four lidars were deployed at the Praia airport during SAMUM–2 (Tesche et al., 2011a; Ansmann et al., 2011). The multiwavelength depolarization Raman lidars BERTHA (Backscatter Extinction lidar-Ratio Temperature Humidity profiling Apparatus) of the Leibniz Institute for Tropospheric Research (IfT) (Althausen et al., 2000; Tesche et al., 2009) and MULIS (Multiwavelenth Lidar System) of the

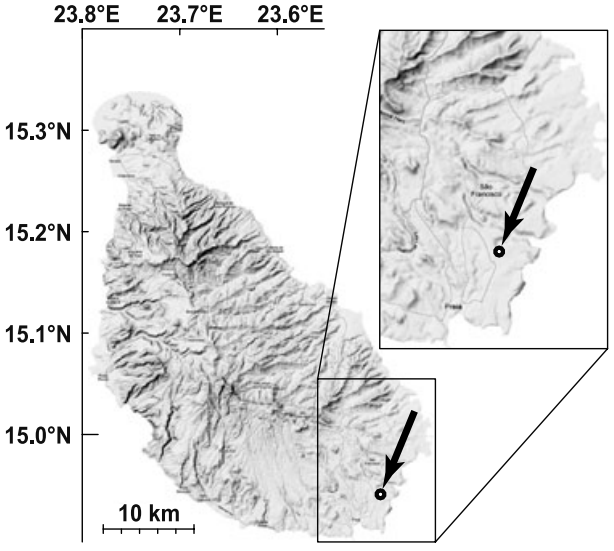

Fig. 1. Map of Santiago island, Cape Verde (http://maps.google.com), location of the lidar station (bullet), and typical wind direction (arrow, 2 m height) in the morning (0900 UTC).

Ludwig-Maximilian University of Munich and the UV portable lidar system (POLIS) also from Munich (Heese et al., 2009; Groß et al., 2011a) were operated in order to study the vertical distribution of aerosol optical properties.

The fourth system was the Doppler wind lidar (WiLi) of IfT. This lidar operates at a wavelength of 2 μm. The lidar measurements are limited to distances greater than about 350 m and strongly depend on the backscattered and Doppler-shifted light from aerosol particles, which act as tracers for the wind velocity. Hence, up to a distance of about 4–5 km the aerosol concentration is the determining factor for analysable signal-to-noise ratios (SNR). At further distances, only liquid or ice cloud particles give sufficient lidar return signals. During SAMUM–2 the lidar was mostly operated with 5 s temporal and 75 m vertical resolution. The system is described in detail by Engelmann et al. (2008) and Engelmann (2010). The overall uncertainty in the determination of the vertical velocity is of the order of 0.10–0.15 m s^{-1} for this system. For further reading on the application of WiLi for BL studies a detailed characterization of updrafts and downdrafts in the atmospheric BL over central Europe can be found in Ansmann et al. (2010).

In addition to vertical measurements the Doppler lidar can be operated in conical-scanning mode in order to obtain horizontal wind vectors. For that, amplitude and phase from sine-wave fits of the line-of-sight velocities determine the wind speed and direction. The method is similar to the vertical-azimuth display (VAD) technique (Browning and Wexler, 1968; Caya and Zawadzki, 1992).

During the campaign, the Doppler lidar was operated mainly for vertical-wind measurements. Only two PPI (plan-position indicator) scans were performed every 30 min in order to determine the horizontal-wind profiles. The first (high) scan operated at a zenith angle of 60° with azimuth stepping of 30° and an integration time of 5 s. The second (low) scan was performed at 75° off zenith with azimuth stepping of 2° and 1 s integration time. The entire scan pattern took about 5 min time. During the remaining 25 min, until the next scan, the lidar was pointed to the zenith and an integration time of 5 s was used. Scans with a zenith angle of 75° allowed measurements down to 150 m whereas with higher scans at 60° altitudes of about 1.5 km could be reached.

Every morning, usually around 1030 UTC (UTC = local time), a Vaisala radiosonde was launched. The radiosonde (type RS–92) measured height profiles of air pressure, temperature, relative humidity, horizontal wind speed and direction up to 15–20 km height. The uncertainties in the Vaisala sonde data are about 1.5 hPa, 0.5 K, 5% and 0.5 m s^{-1} (van As et al., 2006). In Fig. 2, the lidar-derived profiles above ground level (agl) of the horizontal wind component are compared with the RS–92 measurements for 23 and 25 January 2008. The agreement is very good.

In order to check the integrity of the entire set of horizontal wind data which was obtained from the conical lidar scans, we compared these measurements with the wind profiles from the local radiosoundings. From 34 RS–92 ascents during SAMUM–2 we were able to compare 2548 and 2161 data points of wind speed and direction from the high and low Doppler-lidar scans, respectively. Figure 3 shows the correlation between all RS–92 wind profiles and the valid data points from the timely closest lidar scan, that is, the launch of the sonde was within 15 min of the scan. For the comparison the obtained profiles from the scans were linearly interpolated to the heights of the sounding data. The standard deviation between the compared wind direction and wind speed was 23° and 1.0 m s^{-1}, respectively, for the high scans and 14° and 0.9 m s^{-1}, respectively, for the low scans. The major differences were most probably caused by the heterogeneity of the wind field, strong turbulence over the island and the drift-off of the sonde. The few outliers within the wind direction correspond to data points with small wind speeds of less than 1 m s^{-1}.

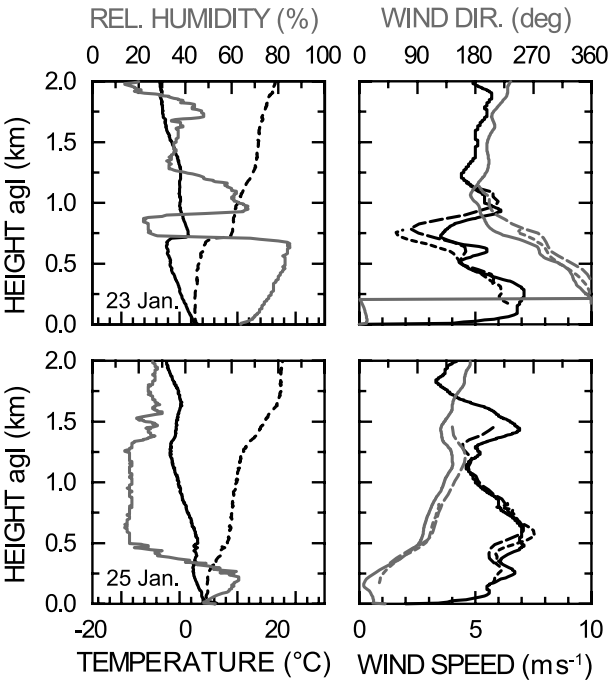

Fig. 2. Left-hand side: Profiles of temperature (solid black) potential temperature (dashed) and relative humidity (grey) from RS–92 radiosoundings at Praia on 23 January, 1800 UTC and 25 January, 1600 UTC. Right-hand side: Comparison of horizontal wind speed (black) and direction (grey) measured with the radiosonde (solid) and the scanning Doppler lidar for the same time periods. The lidar scans were performed for 2 zenith angles of 60° (dashed) and 75° (short dashed).

3. Meteorological data and SAMUM–2 observations

Knippertz et al. (2011) provide a meteorological overview of the SAMUM–2 time period and emphasize three dust phases

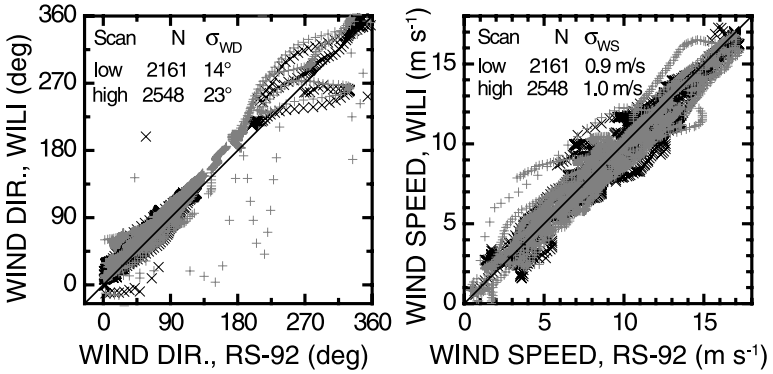

Fig. 3. Correlation of horizontal wind direction (left-hand side) and wind speed (right-hand side) obtained from RS–92 soundings and from conical wind lidar scans at 75° (black ×) and 60° (grey +) zenith angles. Shown are all data points within half an hour of the RS–92 launch measured during SAMUM–2 in January and February 2008.

(17–20 January, 24–26 January and 28 January–2 February 2008) and a phase with clean air in the lowermost 500–1000 m of the troposphere (6–14 February 2008). Complex layering and mixing of maritime aerosol, mineral dust and biomass-burning aerosols (the latter two originating from the African continent) was observed with combination of polarization and multiwavelength Raman lidar and Sun photometers (Groß et al., 2011a,b; Tesche et al., 2011a,b; Toledano et al., 2011). During the dust phases mentioned above mineral dust prevailed from the surface up to 1.0–1.5 km height. The total suspended particle matter at the surface ranged from 250–500 μg m^{-3}, whereas it was below 50 μg m^{-3} for the fourth period in the absence of dust. A layer containing a mixture of biomass-burning smoke and dust was found almost all the time on top of the 1.0–1.5-km dust or maritime layer up to heights of 4–5 km.

Soil and air temperatures have been measured at the field site in addition and are shown in Fig. 4. Two soil temperature sensors were installed 10 m apart and 2 cm deep at places with representative surface conditions for the area. The mean of the two sensors is shown in the plot. Maximum soil temperatures of 43–48 °C and air temperatures at 2 m height of 24–26 °C have been observed during the afternoon. At early morning, air and soil temperatures were almost equal with values of 19–22 °C. The sea surface temperature in the region of Santiago was found to be nearly constant with values of 22–23 °C during January and February 2008 according to Moderate Resolution Imaging Spectroradiometer (MODIS) observations. A 20-K temperature contrast between the soil and the air temperature provides favourable conditions for the development of dust devils and convection plumes (Ansmann et al., 2009b). In fact, several dust devils were observed by eye in close vicinity to the airport on 22 and 23 January 2008. It cannot be excluded that several of these convective elements crossed the lidar site on the two days.

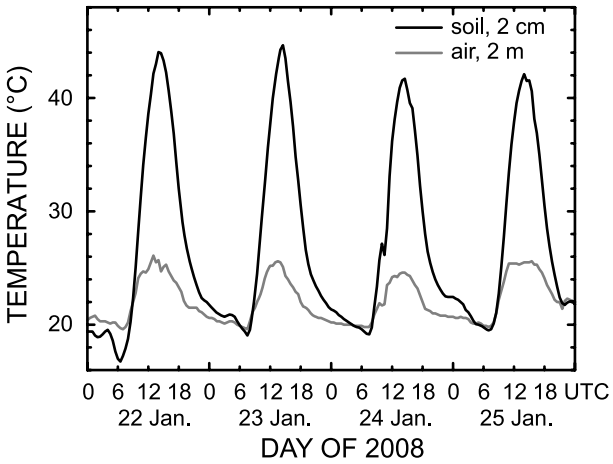

Fig. 4. Soil (at 1–2 cm depth) and air temperature (at 2 m height) measured at the field site (UTC = local time). The soil temperature is the mean of two sensors which were located in representative surface conditions for the area.

4. LES

For a better interpretation of our measurements we used a simple LES setup. LES modelling is not intended to fully reflect and explain the measurements, but to understand the effects of heat islands and dynamic mixing mechanisms in a complementary way. The two islands Santiago and Maio were hence modelled as flat heating surfaces in the ocean, only. More complex modelling including the orography and using a larger domain is planned.

Our newly developed model runs on graphical processor units (GPU, ATI Radeon HD 4870). The GPU model allows us to perform the LES on a 256 × 256 × 64 grid approximately 80 times faster than possible by means of common central processing units (CPU). The model uses a three-step explicit Runge-Kutta integration method with a timesplitting algorithm (e.g. Skamarock and Klemp, 1992; Skamarock et al., 2005) to handle fast waves. Pressure or sound waves are calculated with 1/12 s time integration while advection is calculated with 1 s time steps. Microphysical processes are parameterized using two-moment bulk microphysics based on the scheme of Seifert and Beheng (2006). The model is based on IfT's All-Scale Atmospheric Model (Hinneburg and Knoth, 2005). A detailed description of the new GPU model can be found at its wiki-webpage: http://asamwiki.tropos.de.

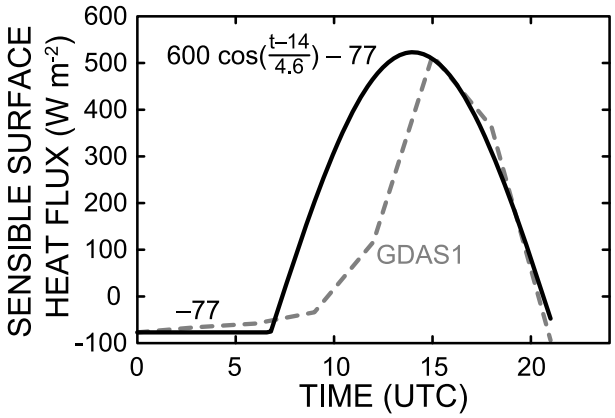

Fig. 5. Diurnal parameterization (t = local time) of the land surface heat flux for the LES. The data were gathered from the GDAS1 archive. See the text for details.

The simulation was performed in a $92 \times 92 \times 3.7\,\mathrm{km}^3$ domain with a horizontal and vertical resolution of 360 m and 60 m, respectively. The initial atmospheric profiles were retrieved from soundings launched at local mid-day.

Because of missing values for the sensible and latent heat fluxes for the soil we used model data of the Global Data Assimilation System (GDAS1) of the United States National Centers for Environmental Prediction. Because the islands are not well resolved by GDAS1 we used data for the nearby continental area in the outbacks of Dakar, Senegal. The surface characteristic is comparable. The applied surface fluxes above the islands were modelled using a diurnal cycle with a maximum of $523\,\mathrm{W\,m^{-2}}$ at 1400 UTC for the sensible heat flux. Figure 5 shows the parameterization compared to the GDAS1 data. We have to keep in mind that the GDAS1 data contain a parameterized BL because of the much lower vertical resolution which appears as an exponential growth in the surface heat flux. In our high-resolution simulations however, the BL is resolved and leads us to the assumption that the surface heat flux is directly proportional to the incoming solar radiation. Hence our parameterization is based on a cosine function with the maximum and drop-off similar to the GDAS1 data. During night the islands are cooled by emission of radiation which is approximated by a negative sensible heat flux of $-77\,\mathrm{W\,m^{-2}}$. The latent heat flux was kept constant throughout the simulation at $55\,\mathrm{W\,m^{-2}}$. Surface heterogeneity of the islands in terms of the heat flux was neglected because apart from a few cities, a limited amount of sugar cane fields, and a few mountain forests most of the two islands are covered by subtropical scrublands.

In order to include surface fluxes at the ocean surface, it is not sufficient to just assume sensible and latent heat fluxes because the development of the MBL needs a very long preliminary upwind domain. The upwind domain between the model boundaries and the islands is certainly too small in our setup. Therefore, a new approach is used for which a second model domain without the islands and with periodic boundary conditions is computed in parallel on a second GPU. Maritime surface fluxes of $90\,\mathrm{W\,m^{-2}}$ sensible heat flux and $20\,\mathrm{W\,m^{-2}}$ latent heat flux are used. The latent heat flux is disturbed by a random noise of $5\,\mathrm{W\,m^{-2}}$ to break the symmetry in the model domain. Subsequently, three cells from the boundary of this periodic domain are used as nesting boundary conditions for the domain containing the islands. In this way, the development of a realistic MBL is realized and more realistic inflow for the island domain is given without the need for a very long fore run range in the upwind region. All model runs start at 0800 UTC and the data shown below are from 1530 UTC.

5. Measurements

Average values of wind speed and direction for the height range from 100–800 m and the daily periods from 1200–2100 UTC are shown in Fig. 6 as well as the daily maximum mixing-layer height. The top of the mixing-layer was determined from the vertical velocity variance (Lenschow and Stephens, 1982; Engelmann et al., 2008; Ansmann et al., 2010) and values between 600 and 1000 m were found at the field site depending on the wind direction and residence time of the air over the heated land surface.

In the following, two cases observed on 23 and 25 January 2008 are compared. On 23 January the prevailing wind direction was north to northwest and the average wind speed was $3–4\,\mathrm{m\,s^{-1}}$. Low wind speeds of $<5\,\mathrm{m\,s^{-1}}$ are favourable for the development of convective plumes (Ansmann et al., 2009b). The air was transported for more than 30 km over the island surface allowing diabatic heating of the air and the island BL to grow.

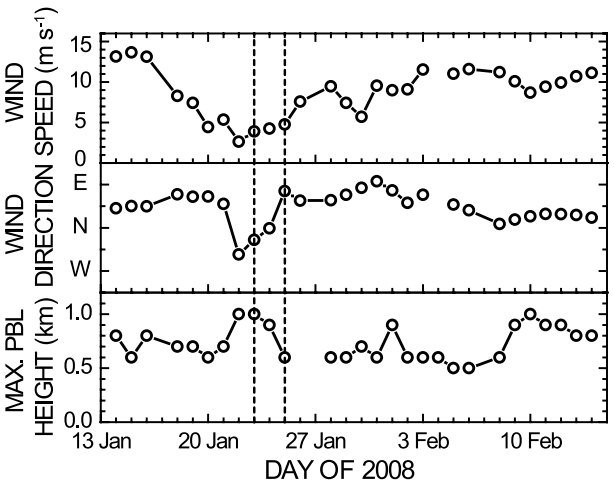

Fig. 6. Top and middle panels: horizontal wind speed and direction within the mixing layer averaged from 100–800 m and from 1200–2100 UTC. Bottom panel: maximum mixing-layer height above ground observed with Doppler lidar at Praia. The two days which we focus on are marked with vertical lines.

From the vertical-wind measurements with the Doppler lidar it was found that the island BL reached a height of 1000 m in the afternoon of that day. In contrast, on 25 January the air masses reached the measurement site directly from the ocean and from easterly directions. So the air was in contact with the island for less than 1–2 km or 3–7 min. The maximum mixing layer height was found to be 0.6 km which is the typical height of the subtropical MBL (e.g. Wood and Bretherton, 2004).

5.1. 23 January 2008. Flow over the hot island

Figure 7 shows the measurements of the Doppler lidar for 23 January 2008. According to the SNR a dust layer with a high particle mass concentration reached up to an altitude of 800 m in the morning. On top of this layer a mixed smoke/dust layer with less total particle mass concentration is visible. The specific classification of these layers was performed by Tesche et al. (2011a) and Knippertz et al. (2011) using polarization lidar measurements and backward-trajectory analysis.

During the course of the day the pure dust layer extended up to 1000 m height and some cumulus clouds developed at the top between 1415 and 1540 UTC. The radiosonde in Fig. 2 shows the island BL top at 1800 UTC. The island BL height had already dropped down to 700 m at that time. The other panels of Fig. 7 depict the vertical and horizontal wind, respectively. Between 1400 and 1600 UTC diabatically heated rising air parcels which sometimes reached updraft velocities of more than 5 m s^{-1} are clearly visible. These high vertical velocities may be related to distinct convective plumes.

Before 1400 UTC and above 600 m height turbulent vertical motions with a scale larger than 0.2 m s^{-1} are not visible. At 1400 and after 1600 UTC coherent structures of up- and downward motions indicate wave activity in regions of stable layering at an altitude of 700–1200 m. Such waves were frequently observed during SAMUM–2. The horizontal wind is shown in the third panel of the figure and was of the order of 4–6 m s^{-1} at the surface. The wind direction turned counter-clockwise from north at the surface over west at 800 m towards south to southwest above 1 km. During the convective period of 1400–1600 UTC momentum (wind speed and direction) was mixed down by turbulence so that the wind speed reached a minimum, and the surface wind direction changed to northwesterly directions in

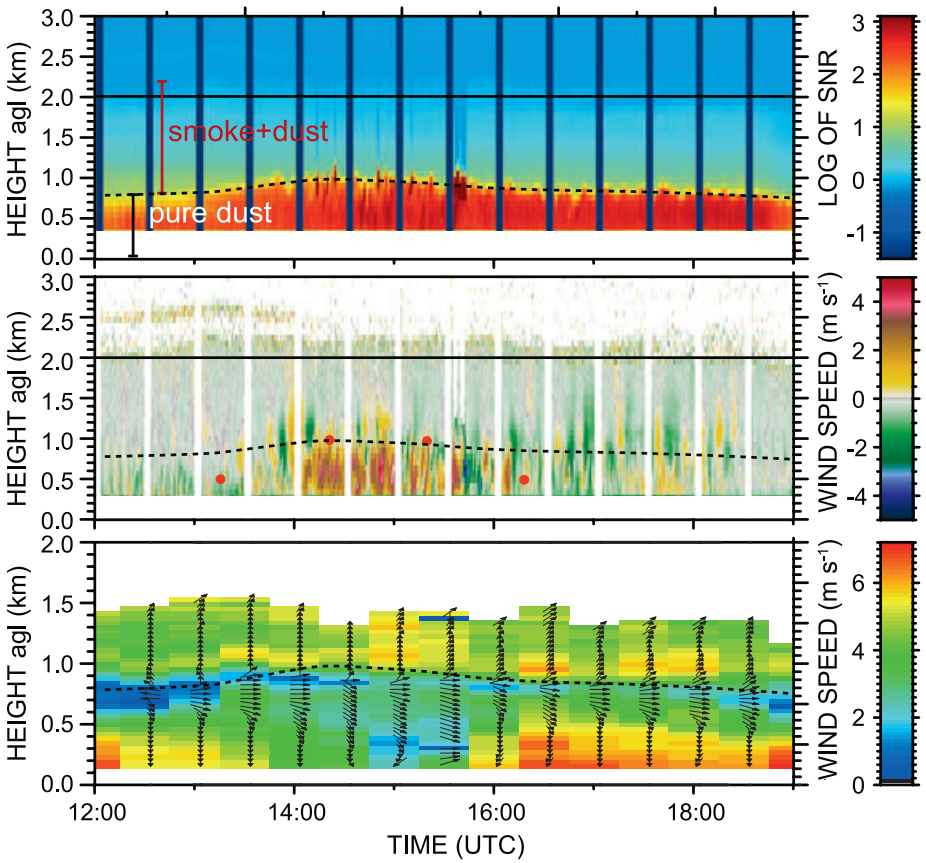

Fig. 7. Doppler lidar observations on 23 January 2008 at Praia, Cape Verde. Temporal developments of the logarithm of the signal-to-noise ratio of the lidar signal (top panel), vertical wind (middle panel) and horizontal wind speed (bottom panel) from 1200–1900 UTC. The resolution of the vertical wind measurements is 5 s and 75 m. Horizontal wind was measured every 30 min, only. The red dots indicate the mixing–layer height, the dashed line the dust-layer height, and the arrows the wind direction.

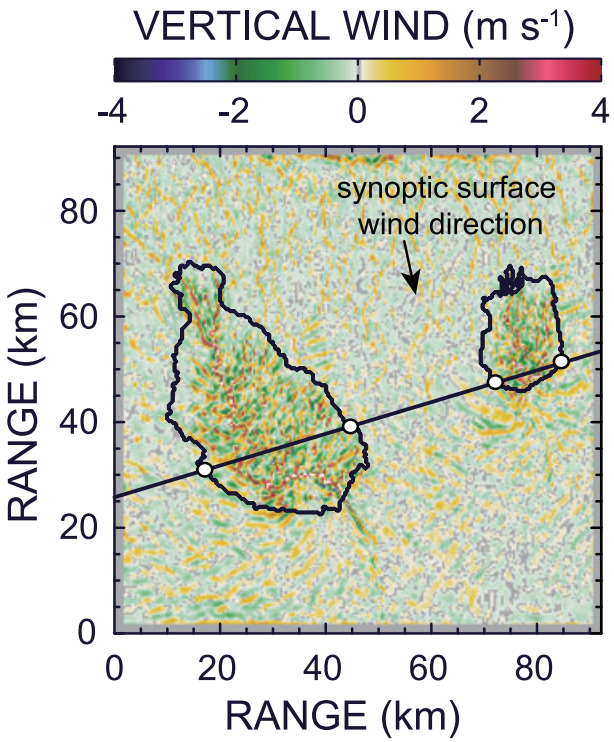

Fig. 8. Vertical wind component over Santiago and Maio derived from LES, for a height of 400 m above sea level and at 1530 UTC on 23 January 2008. For the solid line with circles (indicating the island boundaries) height-distance profiles are shown in Figure 9.

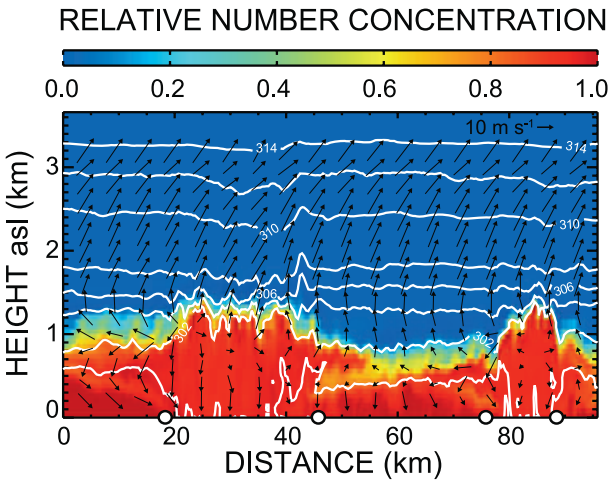

Fig. 9. LES output of the relative number concentration of a passive boundary-layer aerosol tracer, isentropic levels and horizontal wind speed and direction (arrows) at the cut plane indicated in Fig. 8 for 23 January 2008, 1530 UTC. The islands of Santiago and Maio are located from 18–46 km and from 76–88 km, respectively (indicated by open circles). The initial vertical step profile of the tracer at the domain boundaries was 1 up to 700 m height and 0 for heights >700 m.

the afternoon. Consequently, also dust and smoke was mixed down.

We performed LES modelling for 23 January and initialized the model with a radiosounding launched at Praia airport at 1200 UTC before the island BL convection started. As seen in Figs 2 and 7 a strong wind shear was found for the northerly winds at the surface and the southerly flow above. At the height of 800 m the shear was strongest and a minimum of the wind speed was found. The vertical wind field of the LES at 400 m height and at 1530 UTC is shown in Fig. 8. The MBL reaching both islands from the north is heated and thus convective rolls develop already at 5 km inland. Some of these rolls combine and strengthen to more than 4 m s^{-1} updraft velocity, for example, on the southwestern side of Santiago and 10 km inland, others interfere and generate a turbulent island BL, as observed at the field site. Gravity waves are generated around both islands in this simulation which are caused by the strong temperature inversion and the wind shear on the top of the MBL and island BL. In the simulation, these waves are induced within the air parcels with northerly flow over and especially at the south side of the islands and then travel back to the north at higher altitudes with the southerly flow. The occurrence of the waves is consistent with the Doppler lidar measurements (cf. Fig. 7, centre, around 1000 m height where green and yellow colours change periodically).

We included a step profile for a passive tracer in the model setup which may represent the initial dust layer up to a height of 700 m with a 'relative' concentration of 1.0. This tracer may indicate, for example, 300 μg m^{-3} particle mass concentration. Above, the tracer concentration was set to 0. Fig. 9 shows this tracer on the cut plane which is indicated in Fig. 8. The isentropic levels of constant potential temperature and the horizontal winds are given in addition. Surface heating forces the unstable island BL to grow up to about 1.0–1.2 km height over both islands which is consistent with our lidar observations. Rising air parcels above the islands cause convergence of air at the island surface layers (see Fig. 9, distances from 0 to 15 km and from 65 to 90 km). An interesting effect of the wind shear at the islands boundaries, for example, at distance of 45–55 km and 800 m height in Fig. 9, is the formation of lofted aerosol layers. The aerosol is transported upwards by convection and diverged at higher altitudes, above the MBL. The wind above the MBL then transports these new layers out over the ocean. At the same time, air from the free troposphere is mixed into the island BL because of the convergence zone above the islands surface according to the LES model.

In situ measurements of microphysical, optical and chemical properties of particles were performed onboard the Falcon aircraft (Lieke et al., 2011; Petzold et al., 2011; Weinzierl et al., 2011). Particle-size-resolved and single-particle chemical analysis of the obtained impactor samples were performed with Scanning Electron Microscopy by Lieke et al. (2011).

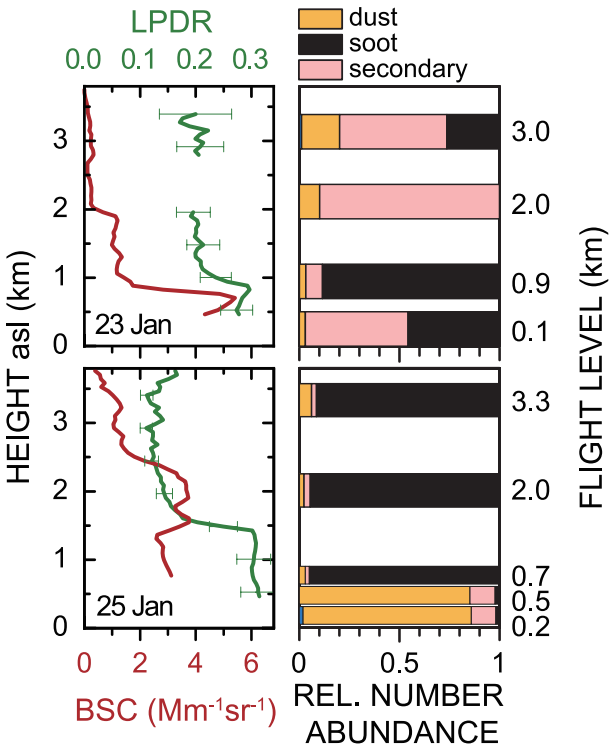

Fig. 10. Left-hand side: Aerosol backscatter coefficient (BSC, red) and linear particle depolarization ratio (LPDR, green) at 532 nm obtained from measurements with BERTHA on 23 January, 1745–1845 UTC and MULIS on 25 January 2008, 1400–1600 UTC, respectively. Right-hand side: Relative particle number abundances of major aerosol species for particles with diameters <500 nm at different altitudes approximately 10–20 km southeast of Praia for the same days around 1600 UTC.

Figure 10 shows the relative particle abundances of the major aerosol species for particles with diameters below 500 nm. The impactor samples were collected above the ocean about 10–20 km southeast of field site. In the small particle size range (particle diameters <500 nm) mainly dust, soot and particles from secondary formation were found. A high amount of smoke particles, which were usually observed above the MBL (Tesche et al., 2011a) was found in the BL on 23 January 2008. No soot was detected at a flight level of 2 km, most probably because this observation was performed above the lofted aerosol layer (see Fig. 10, backscatter profile).

Lidar measurements of the particle backscatter coefficient and linear particle depolarization ratio (LPDR) in Fig. 10 indicate that the optical particle properties were dominated by mineral dust. The high LPDR of 30% is caused by larger coarse-mode particles with diameters >500 nm. The optical properties are dominated by these large dust particles up to a height of around 1000 m, and by a mixture of biomass-burning aerosol and dust above with an LPDR between 15% and 20%. Although advection of soot within the MBL over thousands of kilometres (from southern West Africa to Cape Verde) cannot be ruled out, it appears more likely that most of the soot particles observed close to the surface on 23 January 2008 were mixed downwards locally by the island effects described earlier.

5.2. *25 January. Direct flow from the sea*

On 25 January 2008 typical trade wind patterns prevailed. Figure 11 presents the Doppler lidar observations on that day. The horizontal wind profiles show surface winds of 4–5 m s^{-1} and northeasterly flow (see Fig. 11, bottom panel). The wind speed increased to 6–8 m s^{-1} up to a height of 1500 m and the direction turned to southeast. The radiosonde profile in Fig. 2 (right, bottom panel) shows that the wind turned further clockwise to southwest at altitudes >1.5 km height.

The vertical wind measurements in Fig. 11 (centre panel) indicate a low mixing height of the MBL of 500–600 m, stable layering, and thus no vertical mixing and exchange between the dust layer (<650 m) and the smoke/dust layer (>700 m, see Fig. 10, bottom panels). The measured LPDR of 30% was caused by strongly backscattering coarse-mode dust particles up to 1500 m height. However, a significant amount of smoke particles in terms of number concentration of the fine particle fraction was found from above 700 m height throughout the lofted layers up to above 3000 m height 10–20 km southeast of Praia airport.

As can be seen in Fig. 11 (centre panel), above the MBL, from 500 to 1000 m and from 1000 to 2000 m height persistent features of upward and downward motions of 0.5 and −0.5 m s^{-1}, respectively, occurred on 25 January. These motions were observed for time periods longer than the typical eddy turnover time in the MBL of several minutes. For example between 1345 and 1440 UTC the upward (500–1000 m) and downward motions (1300–2000 m) were most distinct. After 1500 UTC subsidence (green colours in Fig. 11, centre) dominated in the lowermost 2000 m.

LES modelling was performed to better understand these flow patterns. Figure 12 shows the vertical velocity for the 400-m height level at 1530 UTC. Convective rolls develop over Santiago and Maio in this simulation at distances of 5–10 km inland of the east coasts. On first sight, the situation appears to be similar to 23 January. However, caused by the northeasterly winds and sea breeze effects the island BL did not develop over the lidar site on this day. Figure 13 shows the data on the cut plane indicated in Fig. 12. Most interestingly, a defined non-convective 'clear slot' of subsiding air developed about 5 km inland and right above the lidar site (at 45 km in Fig. 13). This feature is rather consistent with the observation in Fig. 11 (centre panel), not only for 25 January, but also for many other days with similar surface winds (see Fig. 6).

On 25 January, the Falcon performed several flights over Santiago island. One of these flight tracks is indicated in Fig. 12 almost parallel to the cut plane of Fig. 13. The 1064-nm backscatter ratio (total-to-Rayleigh backscatter ratio) from

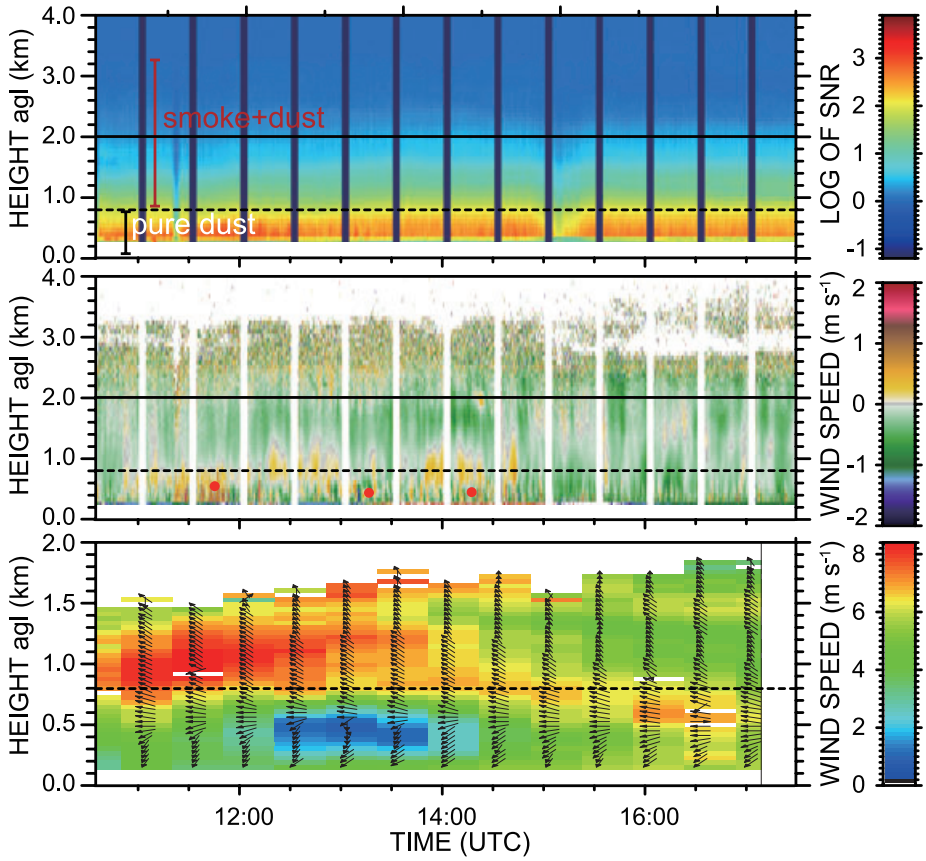

Fig. 11. Same as Fig. 7 but for 25 January 2008.

the aircraft lidar is presented in Fig. 14 for a flight distance of 120 km. On the southeastern side of Santiago the MBL, containing mostly dust and maritime aerosol, is visible up to a height of 500 m. Above 500 m, the mixed layers of biomass-burning aerosol and Saharan dust were found up to 3–4 km height. Following the flight track across the island strong turbulent mixing is visible between 35 and 50 km, caused by diabatic heating of the air after it had passed the island surface for about 10 km. Northwest of the mountain range the graph indicates that the island BL extended up to 1.2 km height and was carried out further downstream with the flow. The flight was extended for approximately 50 km on the open sea. A new MBL developed about 10 km leeward of the island (with cumuli development at the BL top) within the residual island BL whereas the island BL itself slowly decreased down to 800 m at 50 km off the shore. The suppression of the BL development on 25 January may be responsible for the strong gradient in the soot concentration from 500–700 m height shown in Fig. 10.

It is remarkably how well the LES and the Doppler lidar and HSRL measurements agree, even without implementation of orography. It should also be mentioned that the measured radiosonde profiles at Praia and the parameterized surface fluxes were the only input parameters for the LES. Nevertheless, even with the limitations, the LES model clearly indicates the strong influence of the heat islands on the airflow including vertical mixing.

6. Summary and conclusions

Complex layers of maritime, dust and smoke/dust aerosols was observed at the Cape Verde region during SAMUM–2. The comprehensive measurements from several lidar systems and various methods of ground and airborne in situ techniques provided an excellent data set for the analysis of the heat island effect of subtropical islands.

Indications were found that the islands of Cape Verde have a significant effect on vertical mixing between air masses in the MBL and in the free troposphere. Air flow can be significantly disturbed by heat island effects, mainly by surface convection, formation of an island BL and sea-breeze processes.

LES modelling was applied to better interpret the Doppler lidar observations. These preliminary simulations (without considering the orography of the islands) were found in good agreement with the observations and corroborated the

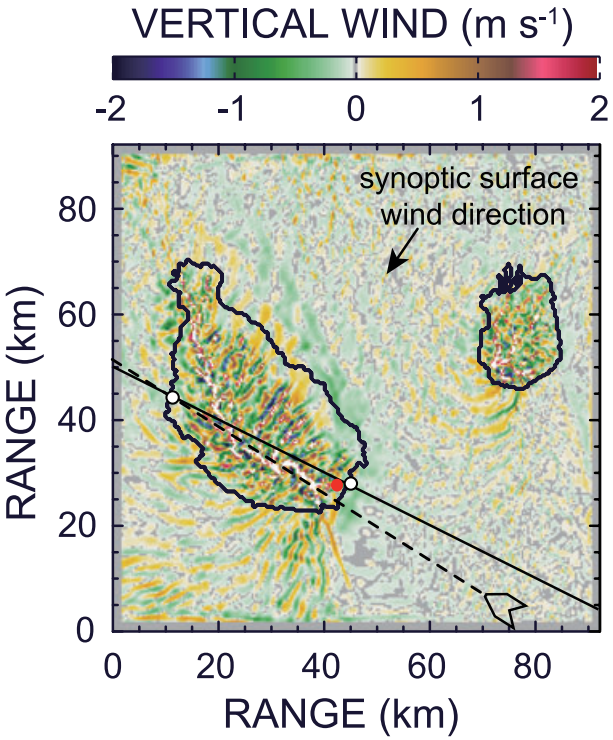

Fig. 12. Same as Fig. 8 but for 25 January 2008, 1530 UTC. The dashed line shows the flight track of the Falcon on 25 January at 1530 UTC (see Fig. 14). The SAMUM–2 super site is marked with the red dot.

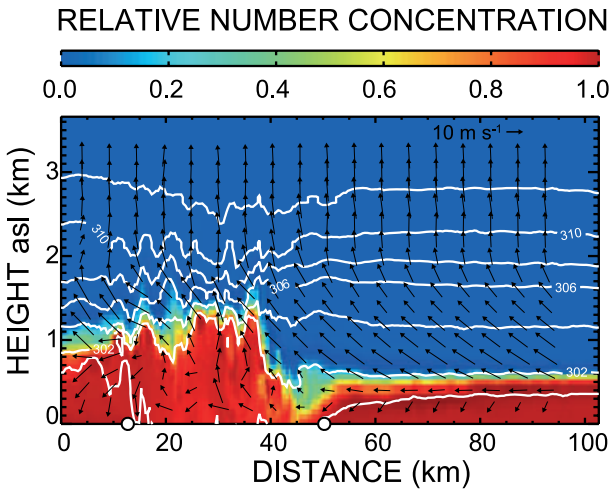

Fig. 13. Same as Fig. 9 but for the cut plane indicated in Fig. 12 for 25 January 2008, 1530 UTC. The island of Santiago is located from 12–50 km on this cut plane. Again, the initial aerosol tracer step function (upwind of both islands) is 1 (red) for heights <700 m and 0 (blue) for heights >700 m.

hypothesis that islands significantly influence downward mixing of aerosols towards the ocean surface. However, for future studies on the SAMUM–2 Doppler lidar data we will implement a Step–Terrain representation (e.g. Gallus and Klemp, 2000) in order to take orographic structures of the islands into account. Furthermore, we will enlarge the LES model towards a greater regime by using several GPUs because especially in Fig. 13 we could not resolve the full extend of the heat plume leeward of Santiago. It should be noted that such fast GPU-based LES models could greatly help to select field sites prior to measurement campaigns.

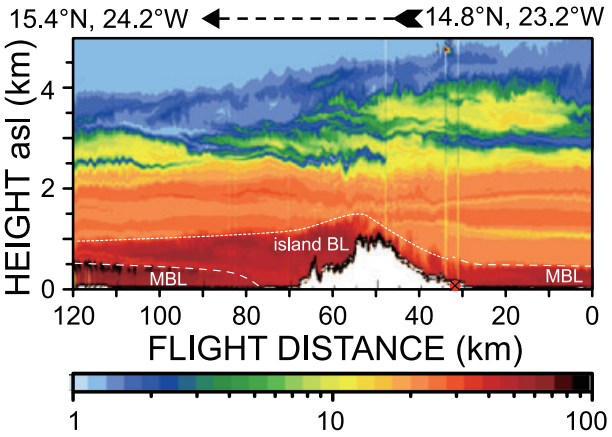

Fig. 14. Height-distance display of the aerosol backscatter ratio (total/Rayleigh backscatter) at 1064 nm measured with HSRL aboard the DLR Falcon research aircraft on 25 January. The aircraft crossed the ground site (red circle at distance 32 km at approximately 1530 UTC). The flight course is shown in Fig. 12.

7. Acknowledgments

The SAMUM research group is funded by the Deutsche Forschungsgemeinschaft (DFG) under grant number FOR 539. The MODIS SST data were obtained from the Physical Oceanography Distributed Active Archive Center (PO.DAAC) at the NASA Jet Propulsion Laboratory, Pasadena, CA. http://podaac.jpl.nasa.gov.

References

Althausen, D., Müller, D., Ansmann, A., Wandinger, U., Hube, H. and co-authors. 2000. Scanning 6-wavelength 11-channel aerosol lidar. *J. Atmos. Oceanic Technol.* **17**, 1469–1482.

Ansmann, A., Tesche, M., Seifert, P., Althausen, D., Engelmann, R. and co-authors. 2009a. Evolution of the ice phase in tropical altocumulus: SAMUM lidar observations over Cape Verde. *J. Geophys. Res.* **114**, D17208, doi:10.1029/2008JD011659.

Ansmann, A., Tesche, M., Knippertz, P., Bierwirth, E., Althausen, D. and co-authors. 2009b. Vertical profiling of convective dust plumes in southern Morocco during SAMUM. *Tellus* **61B**, 340–353.

Ansmann, A., Fruntke, J. and Engelmann, R. 2010. Updraft and downdraft characterization with Doppler lidar: cloud-free versus cumulitopped mixed-layer. *Atmos. Chem. Phys.* **10**, 7845–7858.

Ansmann, A., Petzold, A., Kandler, K., Tegen, I., Wendisch, M. and co-authors. 2011. Saharan Mineral Dust Experiments SAMUM–1 and SAMUM–2: what have we learned? *Tellus* **63B**, this issue.

van As, D., van den Broeke, M. and Helsen, M. 2006. Structure and dynamics of the summertime atmospheric boundary layer over the Antarctic Plateau: 1. Measurements and model validation. *J. Geophys. Res.* **111**, D07102, doi:10.1029/2005JD006956.

Browning, K. A. and Wexler, R. 1968. The determination of kinematic properties of a wind field using Doppler radar. *J. Appl. Meteorol.* **7**, 105–113.

Carbone, R. E., Wilson, J. W., Keenan, T. D. and Hacker, J. M. 2000. Tropical island convection in the absence of significant topography. Part I: life cycle of diurnally forced convection. *Mon. Weather Rev.* **128**, 3459–3480.

Carlis, D. L., Chen, Y.-L. and Morris, V. R. 2010. Numerical simulations of island-scale airflow over Maui and the Maui vortex under summer trade wind conditions. *Mon. Weather Rev.* **138**(7), 2706–2736.

Caya, D. and Zawadzki, I. 1992. VAD analysis of nonlinear wind fields. *J. Atmos. Oceanic Technol.* **9**, 575–587.

Engelmann, R. 2010. *Aerosol vertical exchange in the convective planetary boundary layer: Turbulent particle flux measurements with combined wind and aerosol lidar*, PhD Thesis, University of Leipzig, Germany, 135 pp.

Engelmann, R., Wandinger, U., Ansmann, A., Müller, D., Žeromskis, E. and co-authors. 2008. Lidar observations of the vertical aerosol flux in the planetary boundary layer. *J. Atmos. Oceanic Technol.* **25**(8), 1296–1306.

Esselborn, M., Wirth, M., Fix, A., Tesche, M. and Ehret, G. 2008. Airborne high spectral resolution lidar for measuring aerosol extinction and backscatter coefficients. *Appl. Opt.* **47**(3), 346–358.

Gallus, W. A. and Klemp, J. B. 2000. Behavior of flow over step orography. *Mon. Weather Rev.* **128**, 1153–1164.

Groß, S., Tesche, M., Freudenthaler, V., Toledano, C., Wiegner, M. and co-authors. 2011a. Characterization of Saharan dust, marine aerosols and mixtures of biomass burning aerosols and dust by means of multi-wavelength depolarization and Raman lidar measurements during SAMUM–2. *Tellus* **63B**, this issue.

Groß, S., Gasteiger, J., Freudenthaler, V., Wiegner, M., Geiß, A. and co-authors. 2011b. Characterization of the planetary boundary layer during SAMUM–2 by means of lidar measurements. *Tellus* **63B**, this issue.

Heese, B., Althausen, D., Dinter, T., Esselborn, M., Müller, T. and co-authors. 2009. Vertically resolved dust optical properties during SAMUM: Tinfou compared to Ouarzazate. *Tellus B* **61**, 195–205.

Hinneburg, D. and Knoth, O. 2005. Non-dissipative cloud transport in Eulerian grid models by the volume-of-fluid (VOF) method. *Atmos. Environ.* **39**(23–24), 4321–4330.

Knippertz, P., Tesche, M., Heinold, B., Kandler, K., Toledano, C. and co-authors. 2011. Dust mobilization and aerosol transport from West Africa to Cape Verde: a meteorological overview of SAMUM–2. *Tellus* **63B**, this issue.

Lenschow, D. and Stephens, P. 1982. Mean vertical velocity and turbulence intensity inside and outside thermals. *Atmos. Environ. (1967)* **16**(4), 761–764.

Lieke, K., Kandler, K., Scheuvens, D., Emmel, C., von Glahn, C. and co-authors. 2011. Particle chemical properties in the vertical column based on aircraft observations in the vicinity of Cape Verde islands. *Tellus* **63B**, this issue.

Minda, H., Furuzawa, F. A., Satoh, S. and Nakamura, K. 2010. Convective boundary layer above a subtropical island observed by C-band radar and interpretation using a cloud resolving model. *J. Meteorol. Soc. Japan* **88**(3), 285–312.

Petzold, A., Veira, A., Mund, S., Esselborn, M., Kiemle, C. and co-authors. 2011. Mixing of mineral dust with urban pollution aerosol over Dakar (Senegal): impact on dust physico-chemical and radiative properties. *Tellus* **63B**, this issue.

Savijärvi, H. and Matthews, S. 2004. Flow over small heat islands: a numerical sensitivity study. *J. Atmos. Sci.* **61**(7), 859–868.

Seifert, A. and Beheng, K. D. 2006. A two-moment cloud microphysics parameterization for mixed–phase clouds. Part I: model description. *Meteorol. Atmos. Phys.* **92**, 45–66.

Skamarock, W. C. and Klemp, J. B. 1992. The stability of time-split numerical methods for the hydrostatic and the nonhydrostatic elastic equations. *Mon. Wea. Rev.* **120**, 2109–2127.

Skamarock, W. C., Dudhia, J., Gill, D., Barker, D., Wei, W. and Powers, J. 2005. A description of the advanced research WRF version 2, Technical Report NCAR Tech. Note NCAR/TN-468+STR, National Center for Atmospheric Research, Boulder, CO. 88 pp.

Tesche, M., Ansmann, A., Müller, D., Althausen, D., Mattis, I. and co-authors. 2009. Vertical profiling of Saharan dust with Raman lidars and airborne HSRL in southern Morocco during SAMUM. *Tellus* **61B**, 144–164.

Tesche, M., Groß, S., Ansmann, A., Müller, D., Althausen, D. and co-authors. 2011a. Profiling of Saharan dust and biomass-burning smoke with multiwavelength polarization Raman lidar at Cape Verde. *Tellus* **63B**, this issue.

Tesche, M., Müller, D., Groß, S., Ansmann, A., Althausen, D. and co-authors. 2011b. Optical and microphysical properties of smoke over Cape Verde inferred from multiwavelength lidar measurements. *Tellus* **63B**, this issue.

Toledano, C., Wiegner, M., Groß, S., Freudenthaler, V., Gasteiger, J. and co-authors. 2011. Optical properties of aerosol mixtures derived from sun–sky radiometry during SAMUM–2. *Tellus* **63B**, this issue.

Weinzierl, B., Sauer, D., Esselborn, M., Petzold, A., Veira, A. and co-authors. 2011. Microphysical and optical properties of dust and tropical biomass burning aerosol layers in the Cape Verde region: an overview of the airborne in-situ and lidar measurements during SAMUM–2. *Tellus* **63B**, this issue.

Wood, R. and Bretherton, C. S. 2004. Boundary layer depth, entrainment, and decoupling in the cloud-capped subtropical and tropical marine boundary layer. *J. Clim.* **17**(18), 3576–3588.